Robotica (2006) volume 24, pp. 385–400. © 2006 Cambridge University Press
doi:10.1017/S0263574705002390 Printed in the United Kingdom

Observer-based control of a walking biped robot without orientation measurement

V. Lebastard, Y. Aoustin* and F. Plestan

IRCCyN, LIMR 6597 Ecole Centrale de Nantes, CNRS, Université de Nantes BP 92101,
1, *rue de la Noë, 44321 Nantes cedex 3 (France)*

(Received in Final Form: September 21, 2005, first published online 23 January 2006)

SUMMARY
Two observers based on high order sliding mode approach are proposed to determine the absolute orientation of a walking biped robot without feet. Contrary to velocities observers which have been often designed for robot control, very few works have been proposed for the orientation estimation: in this paper, the estimation of all state variables are derived from *only* the actuated joint variables. Then the technology problem of the absolute measurement is avoided. This latter point is an original contribution of this paper. The observers and the control law converge in finite-time and are well adapted for analysis of the cyclic walking gait. Then, a second original contribution consists in adapting an existing "simplified" Poincaré's sections-based analysis of the stability of the walking to nonlinear systems with not fully available state variables.

KEYWORDS: Walking robot; Orientation measurement; Velocities observers.

I. INTRODUCTION

The legged robots have attracted the interest of many researchers for several decades. Vukobratovic[1] proposed for the first time the well-known Zero-Moment Point (*ZMP*) in 1968, for the synthesis of walking gaits for bipeds.[2,3] In 1977, optimal trajectories[4] are designed for a bipedal locomotion using a parametric optimization. Formal'sky[5] completely characterized the locomotion of anthropomorphic mechanisms in 1982. Sutherland and Raibert[6] proposed their principle of virtual legs for walking robots in 1983.

The previously mentioned works are still used and adapted to more complex legged robots. Honda biped[7] and HRP2 biped[8] (Humanoïd Robotics Project 2), which are probably, on the technological point-of-view, the most advanced biped robots, used the *ZMP* principle for their locomotion in 3D. Parametric optimization is used for walking and running reference trajectories design for a biped robot and non-actuated ankles quadruped one.[9,10]

To our best knowledge, the main applications (handling, transport, . . .) of legged robots are currently limited to the family of the statically stable robots as hexapod, quadruped, . . . The walking gaits of this family of robots is clumsy and slow. The limited use of nimble legged robots, which are dynamically stable, can be explained by the difficulties to define reference trajectories, to design control laws and to ensure the stability of the walking/running. These difficulties have several reasons: the constraints with the ground, which are unilateral, are difficult to analyze:[11] the legged robots can loose contact with the ground during its displacement, or at the impacts; the tip of its stance feet can slide; the ground is not always regular, horizontal, . . . The problem of stability, connected with the gravity effects, of the legged robot must also be taken into account, as the autonomy in terms of energy. In order to overcome these difficulties, with dynamically stable legged robots, the bipeds are the object of many research works because there are well-adapted to the human environments. Trajectories are proposed for the walking of a biped robot, which is dynamically stable, in order to minimize the energy criteria[9,12,13] and to improve the robot behavior. Walking reference trajectories,[14] based on an inverted pendulum model, are checked on *Aibo*, the Sony's dog robot, which is walking on its rear legs, as a biped with non-actuated ankles. The objective consists in starting from a stopped position and in reaching a cyclic gait. Another key point is the effect of the gravity on the bipedal walking: an accurate analyze of gravity for an experimental planar biped with five links, but with non-actuated ankles, *Rabbit*[15] is done for a dynamically stable gait composed of single-support phases and passive impacts. A control law based on the zero dynamics equation is proposed.

In conclusion, the design of reference trajectories and control laws of biped robots, is a still challenging problem and will be not properly solved as long as the dynamics of the under interest robots is not thoroughly understood. Furthermore, the improvement of desired performances induces that the complexity of the control, based on the nonlinear model of the biped robots and using all their state coordinates, increases. Accurate sensors are necessary to measure the joint variables, the absolute orientation of a legged robot, the ground reactions. Unfortunately, a precise measurement of the absolute orientation of a walking robot in single support for example is, by a technical point-of-view, quite difficult to get. For example, in a joint variable usually, a gearbox reducer leads to a more important accuracy of the encoder sensor, directly connected with the output axe of the actuator, to measure the joint angle.

* Corresponding author: E-mail: yannick.Aoustin@irccyn.ec-nantes.fr

Then, there is a real interest to develop observers in order to estimate absolute angular positions and velocities from only the knowledge of the relative angular variables. To our best knowledge, very few works have been done for the design of such observers, the previous works on observers design being done especially for the estimation of velocities (for noiseless differentiation) by supposing that all the angular variables are measured.[16] A first attempt on the design of observer/controller using only the measurement of joint link angular variables (relative angles) for a three-link biped with no actuator in the ankles, in both cases of its stabilization in a vertical position and its walking, has been made by the authors and is based on high gain observers.[17] This class of observers[18] is based on the concept of *uniform observability*[19] of nonlinear systems and their principle consists in reducing the effects of the nonlinear terms in the estimation error equation with a high gain correction. This approach gives an asymptotic convergence observer. Due to this latter property, no controller-observer superposition stability proof has been proposed: this proof is very difficult to establish for nonlinear systems for which the used observers are not finite-time convergent. An estimation of the absolute orientation of a two link biped[20] without foot with a Kalman filter is done. Kalman and his co-authors[21] designed an extended stochastic filter by linearizing the nonlinear system around the current state estimate.

The finite-time convergence property is one of the main characteristics of sliding mode observers (with robustness of estimation/observation versus uncertainties)[22] whose dynamics depend on discontinuous output terms. However, this class of observers presents the main drawback of sliding mode, the *chattering effect* as the estimation error dynamics directly depend on a discontinuous function. This phenomena could generate high-frequency oscillations on observation, which could be negative for the control and the system. In the control context, in order to avoid this problem, in the 90's, a solution has been given through the higher order sliding mode, which removes the sliding mode restrictions (chattering) while preserving its features (robustness, finite-time convergence) and improving the accuracy: in fact, the system dynamics do not directly depend on a discontinuous function. As standard sliding modes, higher order sliding mode approach has been used to design observers. Second order sliding mode observer, based on the twisting algorithm,[23] is designed for an electrical motor:[24] its robustness and its finite-time convergence are proved. A step-by-step higher order sliding mode observer[25] ensures, step-by-step, the finite-time convergence of the estimation error to zero.

The current paper proposes two observer-based controllers of a three link biped, supposing that only the joint variables are available. To design this three-link biped, the physical parameters of a biped prototype *Rabbit*, which is a five link biped, are used. The originality of the present work is double:

- The observers are not only velocities observers, but also absolute position observers. Furthermore, two kinds of finite time convergent observers are used to solve this observation problem.
- An important point of this work consists in the proof of the orbital stability of the biped walking. Original observers, based on second-order sliding mode control,[23] are used. Coupled with a finite-time convergence controller, the use of this class of observers induces an extension of the Poincaré's sections in one dimension[26] for the stability of a biped gait with impulsive impact in the case where all the state is not available.

The article is organized as follows: the dynamical model of the robot is presented in Section II. The control law is presented in Section III. Section IV is devoted to the observation problem. Definition of observability given in Subsection IV.1. A second order sliding mode observer, based on the *twisting algorithm*, with its associated canonical form in order to estimate the absolute orientation of the biped, is detailed in Subsection IV.2, as the asymptotic stability of the walking gaits. An alternative observer needing only the angular variables is presented in Subsection IV.3. Section V contains our conclusion and perspectives. An appendix is added to give the matrices of the dynamic model in single support and impact equations for the studied biped.

II. MODEL OF THE BIPED ROBOT

The complete model of the biped robot consists in two parts: the differential equations describing the dynamics of the robot during the swing phase (these equations are derived using Lagrange's method), and an impulse model of the contact event (the impact between the swing leg and the ground is modelled as an impulsive impact between two rigid bodies.[27])

II.1. Swing motion equations

A planar three-link biped is considered (see Figure 1) and is composed by a torso and two identical legs without knee and foot. The joint between the torso and each leg is actuated by an actuator located in the hip. Then, the biped is underactuated in single support. The dynamic model is given by the following Lagrange equations

$$D_e\ddot{q}_e + H_e\dot{q}_e + G_e = B_e\Gamma + D_R R \tag{1}$$

with $q_e := [q^T\ x_t\ z_t]^T$ (the notation "T" means transposition). Vector q is composed by the joint variables and the absolute orientation of the torso, $q := [\delta_1\ \delta_2\ \psi]^T$, and (x_t, z_t) are the Cartesian coordinates of the center of mass of the torso (see Figure 1). $D_e(q)(5 \times 5)$ is the symmetric positive inertia matrix. Matrix $H_e(q,\ \dot{q})(5 \times 5)$ is the Coriolis and centrifugal effects matrix and $G_e(q)(5 \times 1)$ is the gravity effects vector. B_e is a constant 5×2-matrix composed of 1 and 0 and $D_R(q_e)$ is the 5×2-Jacobian matrix converting the external forces into the corresponding joint torques. $\Gamma = [\Gamma_1\ \Gamma_2]^T$ are the actuators torques. $R = [R_{N1}\ R_{T1}\ R_{N2}\ R_{T2}]^T$ represents the ground reaction acting on the swing/stance leg tips. Assume that

H$_1$ During the swing phase of the motion, the stance leg is acting as a pivot; the contact of the swing leg with the ground results in no rebound and no slipping of the swing leg.

https://doi.org/10.1017/S0263574705002390 Published online by Cambridge University Press

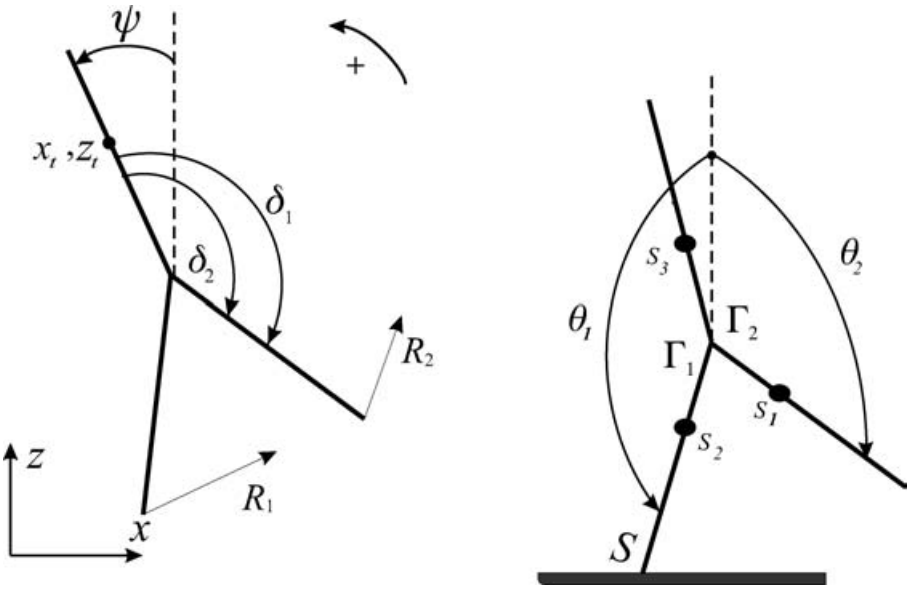

Fig. 1. Three-link biped's diagram: generalized coordinates, torques, forces applied to the leg tips.

Then, Equation (1) can be simplified and rewritten as

$$D\ddot{q} + H\dot{q} + G = B\Gamma \tag{2}$$

As the kinetic energy of the biped is invariant under a rotation of the world frame,[28] and viewed that ψ defines the orientation of the biped, the 3×3-symmetric positive inertia matrix is independent of this variable, *i.e.* $D = D(\delta_1, \delta_2)$, $H(q, \dot{q})(3 \times 3)$ is the Coriolis and centrifugal effects matrix, and $G(q)(3 \times 1)$ is the gravity effects vector. $B(3 \times 2)$ is a constant matrix composed of 1 and 0. Matrices D, H, G, and B are given in Appendix A. Equation (2) can be written as the nonlinear state system

$$\begin{aligned} \dot{x} &:= \begin{bmatrix} D^{-1}(-H\dot{q} - G + B\Gamma) \\ \dot{q} \end{bmatrix} \\ &=: f(x) + g(q_{rel}) \cdot \Gamma \end{aligned} \tag{3}$$

with $x := [\dot{q}^T, q^T]^T = [\dot{\delta}_1\, \dot{\delta}_2\, \dot{\psi}\, \delta_1\, \delta_2\, \psi]^T$ and $q_{rel} := [\delta_1\, \delta_2]^T$ the relative angles. The state space is taken such that $x \in \mathcal{X} := \{x := [\dot{q}^T, q^T]^T \mid \dot{q} \in \mathcal{N},\ q \in \mathcal{M}\}$, where $\mathcal{N} = \{\dot{q} \in \mathbb{R}^3 \mid |\dot{q}| < \dot{q}_M < \infty\}$ and $\mathcal{M} = (-\pi, \pi)^3$. From these definitions, note that all the state variables are bounded.

II.2. Passive impact model

The impact occurs at the end of a single-support phase, when the swing leg tip touches the ground. Let T_I denote impact time. State the subscripts 2 for the swing leg and 1 for the stance leg during the single-support phase. An impact occurs when angle δ_2 equals a desired value δ_{2f} and when the swing leg touches the ground, *i.e.* $x \in \mathcal{S} = \{x \in \mathcal{X} \mid z_2(q) = 0\}$. The term $z_2(q)$ is the altitude of the swing leg. Assume that

- $\mathbf{H}_2$ The impact is passive and absolutely inelastic,
- $\mathbf{H}_3$ The swing leg touching the ground does not slip and the previous stance leg takes off the ground.
- $\mathbf{H}_4$ At the impact, the angular positions are continuous, the angular velocities discontinuous.

Given these hypotheses, the ground reactions at the instant of the impact can be considered as impulsive forces acting on only the swing leg (leg 2) and defined by Dirac delta-functions $R_2 = I_{R_2}\Delta(t - T)$, with $R_2 = R_{2N}R_{2T}$ the vector of magnitudes of impulsive[5] reaction for leg 2. Impact equations can be obtained through the integration of (1) for the infinitesimal time from T_I^- (just before the impact) to T_I^+ (just after the impact). The torques supplied by the actuators at the joints and Coriolis and gravity forces have finite values: thus, they do not influence the impact. Consequently, the impact equations can be written as

$$D_e(\dot{q}_e{}^+ - \dot{q}_e{}^-) = D_R I_{R_2} \tag{4}$$

q_e is the configuration of the biped at $t = T_I$ (from $\mathbf{H}_4$, this configuration does not change at the instant of the impact), $\dot{q}_e{}^-$ and $\dot{q}_e{}^+$ are respectively the angular velocities just before and just after the impact. Furthermore, the velocity of the stance leg tip before the impact equals zero

$$[\dot{x}_1(q_e{}^-, \dot{q}_e{}^-)\ \ \dot{z}_1(q_e{}^-, \dot{q}_e{}^-)]^T = 0_{2\times 1} \tag{5}$$

with (x_1, z_1) the Cartesian coordinates of the stance leg tip. The swing leg after the impact becomes the supporting leg. Therefore, its tip velocity becomes zero after the impact

$$[\dot{x}_2(q_e{}^+, \dot{q}_e{}^+)\ \ \dot{z}_2(q_e{}^+, \dot{q}_e{}^+)]^T = 0_{2\times 1} \tag{6}$$

with (x_2, z_2) the Cartesian coordinates of the swing leg tip. The final result is an expression for $x^+ := [\dot{q}^{+T}, q^{+T}]^T$ (state just before the impact) in terms of $x^- := [\dot{q}^{-T}, q^{-T}]^T$ (state just after the impact) (for more details see appendix B), which can be written as[26] $x^+ = \Delta(x^-)$.

https://doi.org/10.1017/S0263574705002390 Published online by Cambridge University Press

II.3. Nonlinear model all over the step

The overall biped model can be expressed as a nonlinear system with impulse effects as

$$\begin{array}{ll} \dot{x} = f(x) + g(q_{rel})\Gamma & x^-(t) \notin \mathcal{S} \\ x^+ = \Delta(x^-) & x^- \in \mathcal{S}. \end{array} \tag{7}$$

where $\mathcal{S} = \{x \in \mathcal{X} \mid z_2(q) = 0\}$.

III. CONTROL LAW

The control for the walking gait[26] consists in maintaining the angle of the torso at some constant value ψ_d and in controlling the swing leg such that it behaves as a mirror image of the stance leg, $\theta_2 = -\theta_1$ (see Figure 1). During the single-support phase, the degree of under-actuation equals one: only two outputs can be driven. Then, the robot gets a walking motion if the controller drives to zero the following outputs $v := [v_1 v_2]^T = [\psi - \psi_d\, \theta_2 + \theta_1]^T =: h(x)$. As the relative degree of each output component equals 2, and using standard Lie derivative notation,[29] one gets $\ddot{v} = L_f^2 h(x) + L_g L_f h(x)\Gamma$. The control consists in decoupling the system and in imposing a desired dynamic response. Note that, in $\mathcal{X}$, the decoupling matrix $L_g L_f h$ never equals zero. The control law Γ is then

$$\Gamma := [L_g L_f h]^{-1}\left[-L_f^2 h + w\right] \tag{8}$$

to get a linear behavior of the output vector: $\ddot{v} = w$. In the present work, the control law w is chosen to be *finite time convergent*, which could be done with, for example, sliding mode approach. The feedback function used in the present work comes from[30]

$$w = \Upsilon(v, \dot{v}) := \frac{1}{\epsilon} \cdot \begin{bmatrix} \Upsilon_1(v_1, \epsilon \cdot \dot{v}_1) \\ \Upsilon_2(v_2, \epsilon \cdot \dot{v}_2) \end{bmatrix}. \tag{9}$$

Each function $\Upsilon_i(v_i, \epsilon \cdot \dot{v}_i)$ $(i = 1, 2)$, is defined as

$$\begin{aligned} \Upsilon_i := & -\text{sign}(\vartheta_i(v_i, \epsilon \cdot \dot{v}_i)) \cdot |\vartheta_i(v_i, \epsilon \cdot \dot{v}_i)|^{\frac{\alpha}{2-\alpha}} \\ & - \text{sign}(\epsilon \cdot \dot{v}_i) \cdot |\epsilon \cdot \dot{v}_i|^{\alpha} \end{aligned} \tag{10}$$

with $\vartheta_i(\cdot) = v_i + \frac{1}{2-\alpha}\text{sign}(\epsilon \cdot \dot{v}_i) \cdot |\epsilon \cdot \dot{v}_i|^{2-\alpha}$ and $0 < \alpha < 1$. The real parameter $\epsilon > 0$ allows the settling time of the controllers to be adjusted.

IV. OBSERVER DESIGN

IV.1. Analysis of observability

Consider the dynamical part of (7), with y, the vector composed of the measured variables $y := [y_1\ y_2\ y_3\ y_4]^T = [\dot{\delta}_1\ \dot{\delta}_2\ \delta_1\ \delta_2]^T$

$$\begin{aligned} \dot{x} &= f(x) + g(y_3, y_4)\Gamma \\ y &=: \underbrace{\begin{bmatrix} 1 & 0 & 0 & 0 & 0 & 0 \\ 0 & 1 & 0 & 0 & 0 & 0 \\ 0 & 0 & 0 & 1 & 0 & 0 \\ 0 & 0 & 0 & 0 & 1 & 0 \end{bmatrix}}_{C} x \end{aligned} \tag{11}$$

with $x \in \mathcal{X}$, $\Gamma \in \mathbb{R}^2$ and $y \in \mathbb{R}^4$. In the biped context, this model describes the swing motion and is studied over one step, *i.e.* for $t \in [T_I^i, T_I^{i+1}[$, with T_I^i (resp. T_I^{i+1}) the initial (resp. final) impact time of the step i. As $g(y_3, y_4)\Gamma$, the *input-output injection* term of (11), is fully known, an observer for (11) can be designed by the following way. With abuse of notation, consider the next nonlinear system, which is the part of (11) without the input-output injection term

$$\begin{aligned} \dot{x} &= f(x) \\ y &= Cx \end{aligned} \tag{12}$$

Let $\mathcal{O}$ denote the generic observability space defined by

$$\mathcal{O} = \tilde{\mathcal{X}} \cap \tilde{\mathcal{Y}}, \tag{13}$$

with $\tilde{\mathcal{X}} = \text{Span}_{\mathcal{K}}\{\text{d}x\}$ and $\tilde{\mathcal{Y}} = \text{Span}_{\mathcal{K}}\{\text{d}y^{(j)},\ j \geq 0\}$. $\text{Span}_{\mathcal{K}}$ is a space spanned over field $\mathcal{K}$ of meromorphic functions of x. Function $y^{(l)}$ denotes the lth time derivative of y.

Definition 1. *System* (12) *is generically observable if* $\dim \mathcal{O} = 6$. ■

This condition is called *Rank condition of generic observability*. In fact, this definition has to be detailed, because the observability property of (12) depends on x. As a matter of fact, the dimension of $\mathcal{O}$ can fail in $\mathcal{X}$. Let $\mathcal{T}$ denote an open set of $\mathcal{X}$ such that the condition of the following definition fulfills.

Definition 2. *System* (12) *is observable if there exist* $\mathcal{T} \subset \mathcal{X}$ *and* 4 *integers* $\{k_1, k_2, k_3, k_4\}$, *called observability indices, such that*

- $k_1 \geq k_2 \geq k_3 \geq k_4$ *and* $\sum_{i=1}^{4} k_i = 6$,
- *The transformation*

$$\Phi(x) := \left[y_1 \ \cdots\ y_1^{(k_1-1)} \ \cdots\ y_4 \ \cdots\ y_4^{(k_4-1)}\right]^T$$

is a diffeomorphism for $x \in \mathcal{T}$, *which is equivalent to*

$$\text{Det}\left[\frac{\text{d}\Phi(x)}{\text{d}x}\right] \neq 0 \text{ for } x \in \mathcal{T}. \tag{14}$$

■

Proposition 1. *There exist* $\mathcal{T} \subset \mathcal{X}$ *and* $[k_1\ k_2\ k_3\ k_4]^T = [2\ 2\ 1\ 1]^T$ *such that system* (12) *is observable for* $x \in \mathcal{T}$. ■

https://doi.org/10.1017/S0263574705002390 Published online by Cambridge University Press

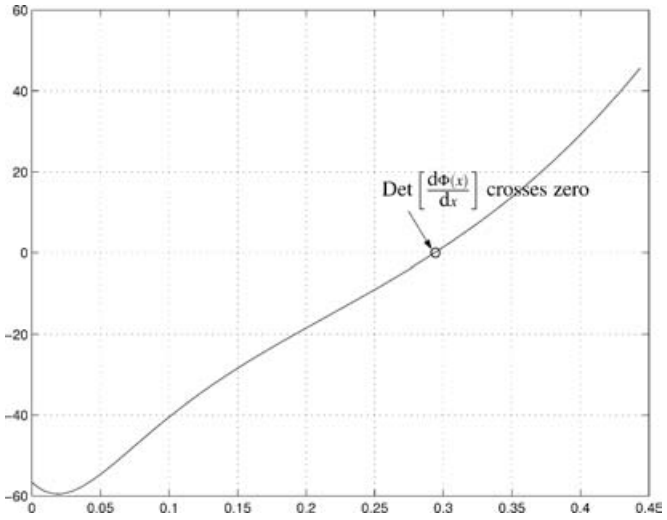

Fig. 2. det($\frac{d\Phi(x)}{dx}$) versus time (sec.) along one step.

Sketch of proof. During the swing phase, and along the desired trajectories, the determinant of $\frac{d\Phi(x)}{dx}$ crosses zero (see Figure 2). At this singular point, system (12) is not observable ($x \in (\mathcal{X}/\mathcal{T})$, the union of $\mathcal{T}$ and $\mathcal{X}$ without their intersection); elsewhere, system (12) is observable ($x \in \mathcal{T} \subset \mathcal{X}$).

IV.2. Second-order sliding mode observer

In this subsection, a second order sliding mode observer[24] is presented. The use of this class of observers is motivated by following reasons. First, as dual properties of sliding mode control, these observers have robustness and finite time convergence properties. Furthermore, the "second order" interest consists in the reduction of chattering phenomenon. Consider system (12) for $x \in \mathcal{T}$. From Proposition 1, system (12) can be rewritten as

$$\dot{z} = \underbrace{\begin{bmatrix} 0 & 1 & 0 & 0 & 0 & 0 \\ 0 & 0 & 0 & 0 & 0 & 0 \\ 0 & 0 & 0 & 1 & 0 & 0 \\ 0 & 0 & 0 & 0 & 0 & 0 \\ 1 & 0 & 0 & 0 & 0 & 0 \\ 0 & 0 & 1 & 0 & 0 & 0 \end{bmatrix}}_{A} z + \underbrace{\begin{bmatrix} 0 \\ \varphi_2(z) \\ 0 \\ \varphi_4(z) \\ 0 \\ 0 \end{bmatrix}}_{\varphi(z)} \qquad (15)$$

$$y = [z_1\ z_3\ z_5\ z_6]^T$$

with $z = [z_1\ z_2\ z_3\ z_4\ z_5\ z_6]^T := [y_1\ \dot{y}_1\ y_2\ \dot{y}_2\ y_3\ y_4]^T = \Phi(x)$.

Observer design

Suppose that there exists a system defined as

$$\dot{\hat{z}} = A\hat{z} + \varphi(\hat{z}) + \chi(\hat{z}, y) \qquad (16)$$

which is an observer of (15), $\hat{z}$ being the estimation of z. Let $\chi(\hat{z}, y)$ denote by $\chi = [0\ \chi_2\ 0\ \chi_4\ \chi_5\ \chi_6]^T$. One uses the standard sliding mode approach for χ_5 and χ_6, which reads as

$$\begin{aligned} \chi_5 &= -\lambda_5 \text{sign}(\hat{z}_5 - z_5) \\ \chi_6 &= -\lambda_6 \text{sign}(\hat{z}_6 - z_6) \end{aligned} \qquad (17)$$

Then, from (16) and (15), the dynamics of estimation errors e_5 and e_6 read as (with $e_j = \hat{z}_j - z_j$, $j = \{5, 6\}$)

$$\begin{aligned} \dot{e}_5 &= e_1 - \lambda_5 \text{sign}(e_5) \\ \dot{e}_6 &= e_3 - \lambda_6 \text{sign}(e_6) \end{aligned} \qquad (18)$$

Then, e_5 and e_6 converge in finite time towards zero if the sliding condition $\dot{e}_j e_j < 0$ ($j = \{5, 6\}$) is fulfilled, *i.e.*

$$\begin{aligned} \lambda_5 &> \text{Max}|e_1| = \text{Max}(|\dot{\hat{\delta}}_1 - \dot{\delta}_1|) \\ \lambda_6 &> \text{Max}|e_3| = \text{Max}(|\dot{\hat{\delta}}_2 - \dot{\delta}_2|) \end{aligned} \qquad (19)$$

Functions χ_2 and χ_4 are defined such that the estimation errors e_1, e_2, e_3 and e_4 converge towards zero in finite-time and read as

$$\begin{aligned} \chi_2 &= -\Lambda_2\ \text{sign}(e_1) \\ \chi_4 &= -\Lambda_4\ \text{sign}(e_3) \end{aligned} \qquad (20)$$

Given that $\dot{e}_1 = e_2$ and $\dot{e}_3 = e_4$, one gets

$$\begin{aligned} \ddot{e}_1 = \dot{e}_2 &= \varphi_2(\hat{z}) - \varphi_2(z) - \Lambda_2\ \text{sign}(e_1) \\ \ddot{e}_3 = \dot{e}_4 &= \varphi_4(\hat{z}) - \varphi_4(z) - \Lambda_4\ \text{sign}(e_3) \end{aligned} \qquad (21)$$

The choice for Λ_2 and Λ_4, based on the *twisting algorithm*,[23] allows to ensure that the previous system converges to zero in finite-time, and then to ensure that e_1, e_2, e_3 and e_4 reach zero. The twisting algorithm ensures this convergence[23,24] (for $j = \{1, 3\}$) if

$$\begin{aligned} \Lambda_{j+1} &= \begin{cases} \lambda_m^{j+1} & \text{if } e_j \dot{e}_j \le 0, \\ \lambda_M^{j+1} & \text{if } e_j \dot{e}_j > 0, \end{cases} \\ \lambda_m^{j+1} &> \text{Max}(|\varphi_{j+1}(\hat{z}) - \varphi_{j+1}(z)|) \\ \lambda_M^{j+1} &> 3\lambda_m^{j+1} \end{aligned} \qquad (22)$$

Then, a second-order sliding mode observer for (11) reads as

$$\dot{\hat{x}} = f(\hat{x}) + g(y_3, y_4)\Gamma + \left[\frac{d\Phi(\hat{x})}{d\hat{x}}\right]^{-1} \chi(\hat{x}, y) \qquad (23)$$

is an observer of (11) with

$$\chi(\hat{x}, y) = \begin{bmatrix} 0 \\ \chi_2 \\ 0 \\ \chi_4 \\ \chi_5 \\ \chi_6 \end{bmatrix} = \begin{bmatrix} 0 \\ \Lambda_2\ \text{sign}(\hat{x}_1 - y_1) \\ 0 \\ \Lambda_4\ \text{sign}(\hat{x}_2 - y_2) \\ \lambda_5\ \text{sign}(\hat{x}_4 - y_3) \\ \lambda_6\ \text{sign}(\hat{x}_5 - y_4) \end{bmatrix} \qquad (24)$$

Remark 1. *As observer* (23) *is based on the second and first orders sliding mode, it is applicable only for observability indices equal to* 1 *or* 2. *This restriction will be lax with the observer designed in Section* IV.3.

Remark 2. *Observer* (23) *is designed for the swing phase. But, a step is composed of both swing and impact phases. At the impact event, the impact model is applied to the estimated*

https://doi.org/10.1017/S0263574705002390 Published online by Cambridge University Press

state.[31] *Then, over one step, an observer of* (7) *reads as*

$$\begin{aligned} \dot{\hat{x}} &= f(\hat{x}) + g(y_3, y_4)\Gamma + \left[\frac{\mathrm{d}\Phi(\hat{x})}{\mathrm{d}\hat{x}}\right]^{-1}\chi(\hat{x}, y) \quad \hat{x}^-(t) \notin \hat{\mathcal{S}} \\ \hat{x}^+ &= \Delta(\hat{x}^-) \qquad\qquad\qquad\qquad\qquad\quad \hat{x}^- \in \hat{\mathcal{S}} \end{aligned} \tag{25}$$

with $\hat{\mathcal{S}} = \{\hat{x} \in \hat{\mathcal{X}} \mid \hat{z}_2(\hat{q}) = 0\}$.

Around the singular point, *i.e.* $x \in (\mathcal{X}/\mathcal{T})$, it is necessary to adapt the observer, which is not valid at exactly the singularity. Two intuitive and quite natural solutions are proposed:

Proposition 2. *For* $x \in (\mathcal{X}/\mathcal{T})$, *observer* (23) *is turned into an estimator when* $\det(\frac{\mathrm{d}\Phi(\hat{x})}{\mathrm{d}\hat{x}}) = 0$, *i.e.*

$$\dot{\hat{x}} = f(\hat{x}) + g(y_3, y_4)\Gamma$$

■

If the observer has not still converged when the singularity appears, there is discontinuity on observer dynamics. In the opposite case, there is no discontinuity viewed that the corrective term of the observer still equals zero. Note that, viewed that the observer is finite-time convergence one, the observer gain can be tuned such that the observer convergence time is smaller than the singularity moment. However, if one gets a high gain, troubles could affect system behavior through high level transients. To avoid the discontinuity appearing in the previous solution, a smooth corrective term is added at the observer.

Proposition 3. *For* $x \in \mathcal{X}$, *observer* (23) *is turned into the dynamic system* (*with* $\Theta \in \mathbb{R}^{6\times 6}$)

$$\dot{\hat{x}} = f(\hat{x}) + g(y_3, y_4)\Gamma + \Theta\chi(\hat{x}, y) \tag{26}$$

with

$$\Theta = \begin{cases} \left[\frac{\mathrm{d}\Phi(\hat{x})}{\mathrm{d}\hat{x}}\right]^{-1} & \text{if } \left|\det\left(\frac{\mathrm{d}\Phi(\hat{x})}{\mathrm{d}\hat{x}}\right)\right| \geq D_{min} \\ & \text{then } \hat{x} \in \mathcal{T} \\ \frac{1}{D_{min}}\left|\det\left[\frac{\mathrm{d}\Phi(\hat{x})}{\mathrm{d}\hat{x}}\right]\right|\left[\frac{\mathrm{d}\Phi(\hat{x})}{\mathrm{d}\hat{x}}\right]^{-1} & \text{if } 0 < \left|\det\left(\frac{\mathrm{d}\Phi(\hat{x})}{\mathrm{d}\hat{x}}\right)\right| < D_{min} \\ & \text{then } \hat{x} \in (\mathcal{X}/\mathcal{T}) \\ 0_{6\times 6} & \text{if } \det\left(\frac{\mathrm{d}\Phi(\hat{x})}{\mathrm{d}\hat{x}}\right) = 0 \\ & \text{then } \hat{x} \in (\mathcal{X}/\mathcal{T}) \end{cases} \tag{27}$$

with D_{min} *a positive real arbitrarily stated by the user.* ■

The choice of D_{min} is made in order that the condition number with respect to inversion of $[\frac{\mathrm{d}\Phi(\hat{x})}{\mathrm{d}\hat{x}}]$ is not "too much large". Of course, this multiplication acts on observer gain values and implies that, around the singular point, the convergence conditions are not satisfied. It means that the singularity area must be "sufficiently small".

IV.2.1. Simulations. The parameters of the five-link biped prototype "Rabbit"[15] are used to design the three-link biped parameters. The masses and lengths of the links (Indices 1, 2, 3: swing leg, stance leg, torso, resp.) are $m_1 = m_2 = 10\,\mathrm{kg}$, $m_3 = 16.3\,\mathrm{kg}$, $l_1 = l_2 = 0.8\,\mathrm{m}$, $l_3 = 0.625\,\mathrm{m}$. The distances between the joint and the mass center of each link are $s_1 = s_2 = 0.279\,\mathrm{m}$, $s_3 = 0.15\,\mathrm{m}$. The inertia moments around the mass center of each link are $I_1 = I_2 = 0.4006\,\mathrm{kg}\cdot\mathrm{m}^2$, $I_3 = 2.0670\,\mathrm{kg}\cdot\mathrm{m}^2$. The inertia of the rotor for each DC motor is $I = 3.32\,10^{-4}\,\mathrm{kg}\cdot\mathrm{m}^2$. The ratio N of the gearbox reducers is equal to 50. Value U of the applied torques equals $150\,\mathrm{N}\cdot\mathrm{m}$. The control law described in Section III is applied with parameters $\alpha = 0.9$ and $\epsilon = 20$ and is coupled to observer (26). The initial real and estimated values have been respectively stated as

$$\begin{aligned} &[\dot{\delta}_1,\ \dot{\delta}_2,\ \dot{\psi},\ \delta_1,\ \delta_2,\ \psi] \\ &\quad = [-1.53,\ 1.53,\ -0.05,\ -2.9374,\ -2.4033,\ -0.6283] \\ &[\dot{\hat{\delta}}_1,\ \dot{\hat{\delta}}_2,\ \dot{\hat{\psi}},\ \hat{\delta}_1,\ \hat{\delta}_2,\ \hat{\psi}] \\ &\quad = [-1.50,\ 1.50,\ 0.00,\ -2.8798,\ -2.3562,\ -0.5236] \end{aligned}$$

Parameters D_{min} has been stated to 5, and the sliding mode observer parameters are $\lambda_m^2 = 10$, $\lambda_M^2 = 50$, $\lambda_m^4 = 10$, $\lambda_M^4 = 50$, $\lambda_5 = 1$, $\lambda_6 = 1$. The choice of observer and control law parameters has been made with respect to closed-loop dynamics and admissible maximum value for input (saturation). Figure 3 displays absolute position ψ and the estimation error $\psi - \hat{\psi}$: the absolute position converges to the desired value ψ_d and the estimation error converges towards zero before each impact. The same remark can be made for the absolute velocity $\dot{\psi}$ and the estimation error $\dot{\psi} - \dot{\hat{\psi}}$ (Figure 4). Figure 5 displays walking over several steps.

IV.2.2. Stability. In this section, the objective is to prove the asymptotic stability of the walking of the biped controlled by controller (8) coupled with observer (26). An important result is that the stability[26] can be proven on the basis of a restriction of the Poincaré's map to a one-dimensional manifold. This section proposed an original extension of this latter result to observer-based controlled systems. As the "real" state vector is not fully measured, the "real" zeros dynamics and impact surface manifolds can not be used in the stability proof, the idea is then to suppose that the estimated state is on "estimated" zeros dynamics and impact surface manifolds. The finite-time convergence of the observer and controller, at the end of the first step, ensures that the estimated manifolds are the same than "real" ones. Then, it is possible to use the standard reduced Poincaré's approach to establish, over the second step, the stability.

Sketch of the stability proof. The stability proof is made over two steps (see Figure 6). The first step consists in making the observer converge to real system before the impact, and also in making the control objectives fulfill before the impact. Then, at the end of the first step, the observer and the controller have converged. During the second step, it is then possible to apply the simplified Poincaré's approach.[26] ■

Notations. The impact time at the end of the ith step is noted T_I^i and is taken as the time origin for the $i+1$th

https://doi.org/10.1017/S0263574705002390 Published online by Cambridge University Press

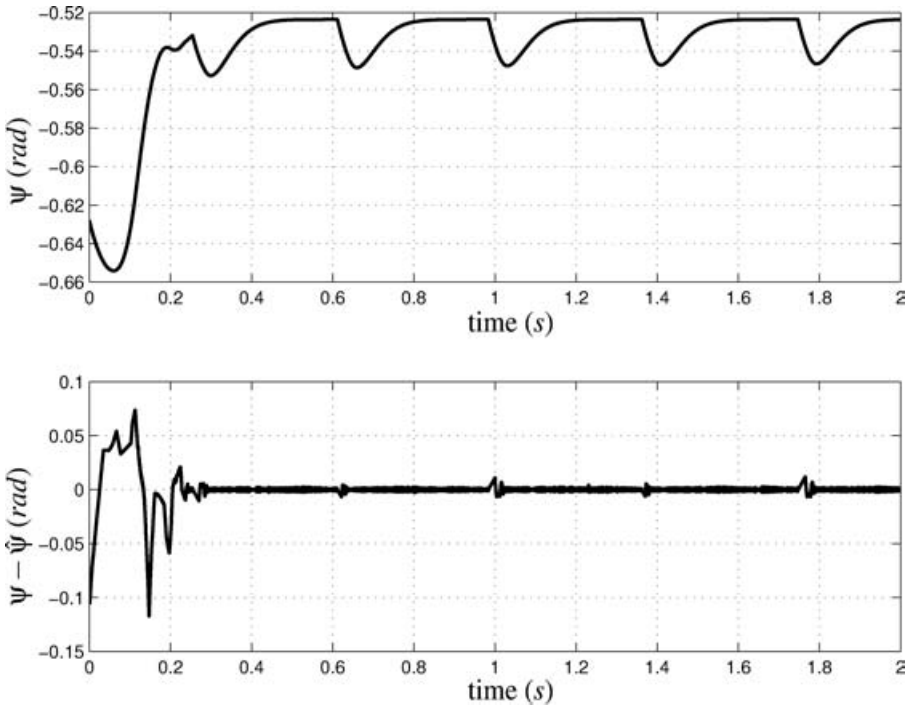

Fig. 3. Absolute orientation ψ (rad) (top) and estimation error $\psi - \hat{\psi}$ (rad) (bottom) versus time (sec.).

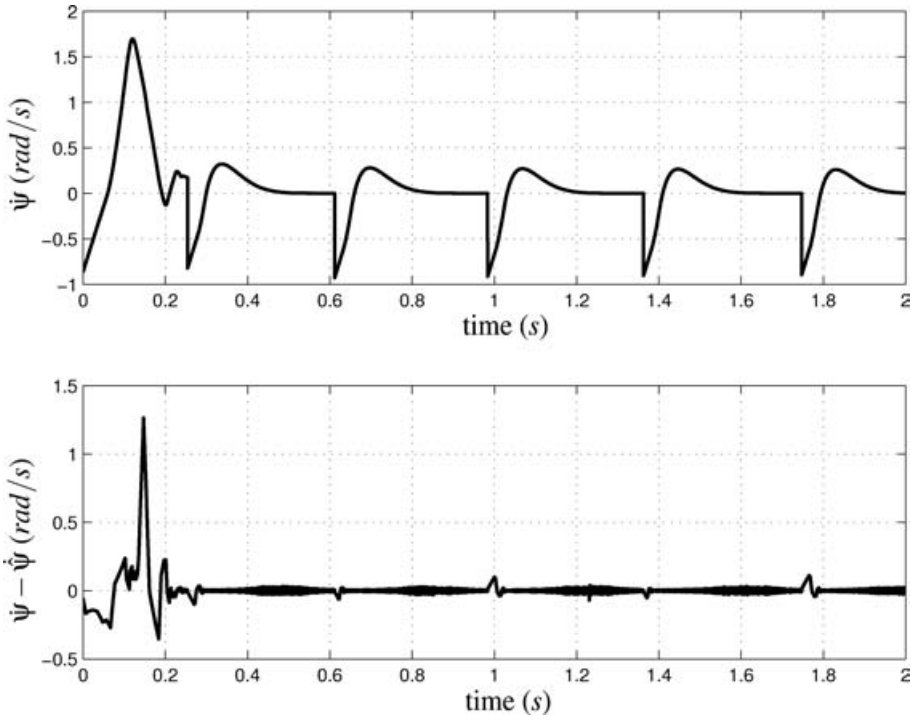

Fig. 4. Absolute velocity $\dot{\psi}$ (rad/s) (top) and estimation error $\dot{\psi} - \dot{\hat{\psi}}$ (rad/s) (bottom) versus time (sec.).

step. Let T_O^i denote the convergence (towards 0) time of the estimation error over the ith step and T_C^i the convergence time of the controller over the ith step. The observer and the controller have been tuned such that $T_O^i \leq T_C^i < T_I^i$, *i.e.* the observer converges faster than the controller over the step i (Figure 6). As the observer converges to real state in finite time, it is obvious that $T_O^i = 0$ for $i > 1$: then, from T_O^i, one has $\hat{x} = x$ (see Figure 6).

Numerical procedure. Let $\hat{Z}$ denote the "estimated" zero dynamics manifold, $\hat{Z} = \{\hat{x} \in \hat{\mathcal{X}} \mid h(\hat{x}) = 0, \dot{h}(\hat{x}) = 0\}$, $\hat{\mathcal{S}}$ the "estimated" impact surface manifold, $\hat{\mathcal{S}} = \{\hat{x} \in \hat{\mathcal{X}} | \hat{\delta}_2 +$

https://doi.org/10.1017/S0263574705002390 Published online by Cambridge University Press

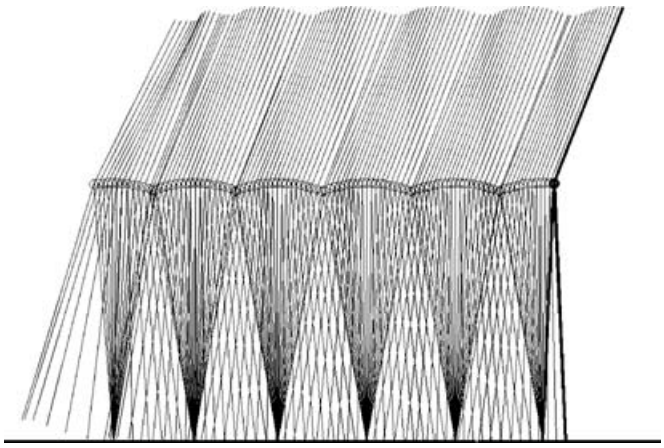

Fig. 5. Plot of walking as a sequence of stick figure.

$\hat{\psi}=\delta_{2f}+\psi_d$ and $\hat{\delta}_1=\delta_{1f}\}$, $\hat{\mathcal{X}}:=\{\hat{x}:=[\dot{\hat{q}}^T, \hat{q}^T]^T | \dot{\hat{q}} \in \mathcal{N}$, $\hat{q} \in \mathcal{M}\}$, $\hat{q}$ and $\dot{\hat{q}}$ being the estimated values of q and $\dot{q}$. The conditions[32] required to define the restricted Poincaré map are:

1. $\hat{\mathcal{S}} \cap \hat{\mathcal{Z}}$ is a smooth sub-manifold of $\hat{\mathcal{X}}$. It is equivalent to the fact that the map

$$\begin{bmatrix} h(\hat{x}) \\ \dot{h}(\hat{x}) \\ \hat{\delta}_2 \end{bmatrix} = \begin{bmatrix} \hat{\psi} - \psi_d \\ \hat{\theta}_1 + \hat{\theta}_2 \\ \dot{\hat{\psi}} \\ \dot{\hat{\theta}}_1 + \dot{\hat{\theta}}_2 \\ \hat{\delta}_2 \end{bmatrix} \tag{28}$$

has constant rank equal to 5 on $\hat{\mathcal{S}} \cap \hat{\mathcal{Z}}$, which is obvious to prove. If $(\dot{\hat{q}}, \hat{q}) \in \hat{\mathcal{S}} \cap \hat{\mathcal{Z}}$, $\hat{q}$ equals a constant, denoted $\hat{q}_0$. Let $\gamma := [h(\hat{x})^T \ \hat{\theta}_1(\hat{x})]^T$ which has full rank at $\hat{q}_0$. On $\hat{\mathcal{Z}}$, one has $\dot{h}(\hat{x}) = 0$

$$\begin{bmatrix} 0 \\ \dot{\hat{\theta}}_1 \end{bmatrix} = \frac{\partial \gamma}{\partial \hat{q}} \dot{\hat{q}} \tag{29}$$

Proposition 4. *Let us define p, a diffeomorphism from $\mathbb{R} \to \hat{S} \cap \hat{Z}$ to complete equation* (29) *with the configuration vector q_0 of the impact such as:*

$$p(\dot{\hat{\theta}}_1) = \begin{bmatrix} \left[\frac{\partial \gamma(\hat{q}_0)}{\partial \hat{q}}\right]^{-1} \dot{\hat{\theta}}_1 \\ \hat{q}_0 \end{bmatrix} \tag{30}$$

2. The decoupling matrix[26] $L_g L_f h(\hat{x})$ is invertible on $\hat{\mathcal{X}}$.
3. The cross section for the Poincaré map will be taken to be $\hat{S}$, the "estimated" impact surface. Define $\lambda : \mathbb{R} \to \mathbb{R}$ computed by the following manner
   - Let $\dot{\hat{\theta}}_1(T_I^0) < 0$ denote the initial estimated angular velocity just before the *initial* impact. Compute $\hat{x}^-(T_I^0) := p(\dot{\hat{\theta}}_1^-(T_I^0))$, the estimated state vector of the robot before the impact. State the real state before the impact as (given that δ_1, δ_2 and the corresponding velocities are measured)

$$x^-(T_I^0) := [\dot{\delta}_1^-(T_I^0)\dot{\delta}_2^-(T_I^0)\ \dot{\psi}^-(T_I^0)\delta_1^-(T_I^0)\delta_2^-(T_I^0)\psi^-(T_I^0)]^T$$
$$x^-(T_I^0) := [y_1^-(T_I^0)y_2^-(T_I^0)\dot{\psi}^-(T_I^0)y_3^-(T_I^0)y_4^-(T_I^0)\psi^-(T_I^0)]^T$$

   - Apply the impact model to $\hat{x}^-(T_I^0)$ (resp. $x^-(T_I^0)$), then we obtain $\hat{x}^+(T_I^0) = \Delta(\hat{x}^-(T_I^0))$ (resp. $x^+(T_I^0) = \Delta(x^-(T_I^0))$).
   - Use $x^+(T_I^0)$ as the initial condition in (7) controlled by (9) which uses $\hat{x}$. Simulate until one of the following happens:
     a) There exists a time T_I^1 for which $\hat{\delta}_2 + \hat{\psi} = \delta_{2f} + \psi_d$ and $T_O^1 \leq T_C^1 < T_I^1 < \infty$, we apply again the impact model to $\hat{x}^-(T_I^1)$, then we obtain $\hat{x}^+(T_I^1) = \Delta(\hat{x}^-(T_I^1))$. At this time, the real and estimated state variables have same values, viewed that the observer has finite-time convergence of estimation error, and that the observer gains have been tuned such that $T_O^1 < T_I^1$. Use $\hat{x}^+(T_I^1)$ as the initial condition in (7) controlled by (9). If there exists a time T_I^2 for which $\hat{\delta}_2 + \hat{\psi} = \delta_2 + \psi = \delta_{2f} + \psi_d$ such that $T_O^2 \leq T_C^2 < T_I^2 < \infty$, then $\lambda[\dot{\hat{\theta}}_1^-(T_I^1)] := \dot{\hat{\theta}}_1^-(T_I^2)$; else $\lambda[\dot{\hat{\theta}}_1^-(T_I^1)]$ is undefined at this point.

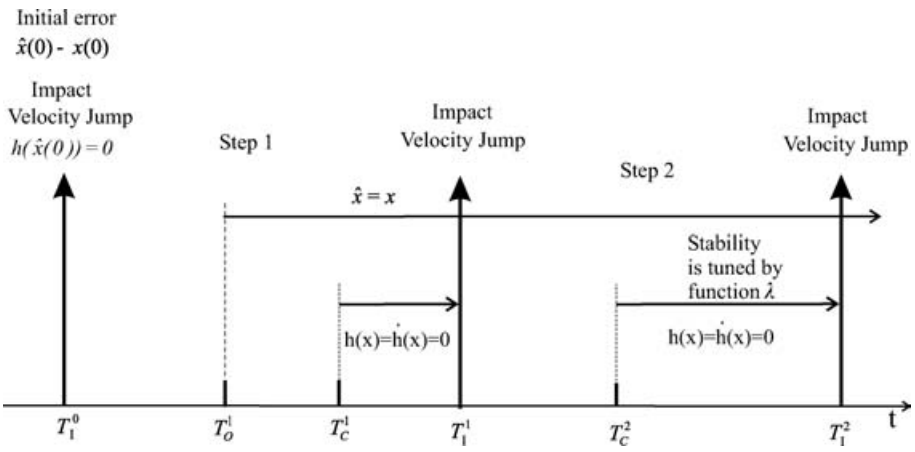

Fig. 6. Scheme defining the observer convergence time T_O^i, the controller convergence time T_C^i, the impact time T_I^i and the behavior of the observer (through the estimation error) and the controller (through the output $h(x)$ and its time derivative), over several steps.

https://doi.org/10.1017/S0263574705002390 Published online by Cambridge University Press

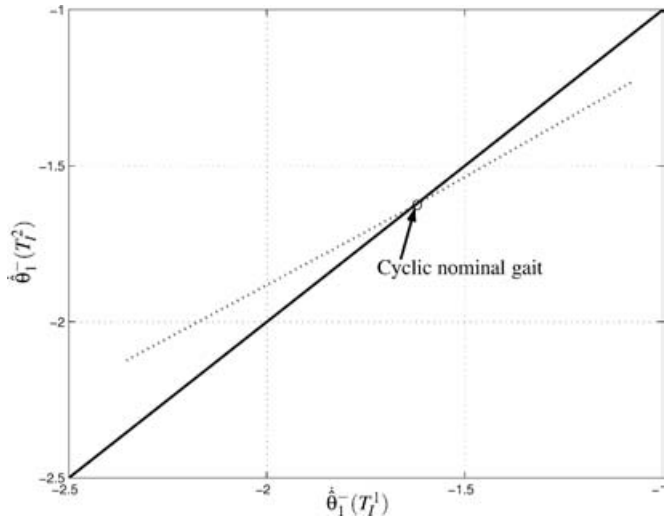

Fig. 7. Function λ (dotted line) and identity function (bold line) versus $\dot{\hat{\theta}}^-(T_I^0)$. This graph describes the existence of an asymptotically stable walking motion.

b) There does not exist a $T_I^2 > 0$ such that $\hat{\delta}_2 + \hat{\psi} = \delta_{2f} + \psi_d$; in this case, it is also true that $\lambda[\dot{\hat{\theta}}_1^-(T_I^1)]$ is undefined at this point.

In order to determine if the closed-loop system is stable, function λ is evaluated for $\dot{\hat{\theta}}_1^-(T_I^0) \in [-3, -0.5]$, $\psi \in [0.8 \cdot \psi_d, 1.2 \cdot \psi_d]$ and $\dot{\psi} \in [-0.1, 0.1]$. Figure 7 displays function $\lambda : \lambda$ is undefined for $\dot{\hat{\theta}}_1^-(T_I^1)$ less than -2.4 rad/s and more than -1.1 rad/s. A fixed point appears at approximately $\dot{\hat{\theta}}_1^-(T_I^1) = -1.63$ rad/s, and corresponds to an asymptotically stable walking cycle. Figure 8 displays $\dot{\hat{\theta}}_1^-(T_I^0)$ in terms of initial estimation errors on unmeasured variables $\psi(T_I^0) \in [0.8 \cdot \psi_d, 1.2 \cdot \psi_d]$ and $\dot{\psi}(T_I^0) \in [-0.1, 0.1]$. For each point of this 3D-area, the estimated state variable converges to real ones, the control outputs reach zero before the end of each step, and the biped converges to a stable limit cycle. In terms of this 3D-area, the asymptotically stable walking cycle corresponds to the star point.

IV.3. Step-by-step observer

In order to reduce the number of sensors or to limit the noise introduced by the differentiation (for computation of velocity), the measurements concern now only the joint variables. Of course, it implies that the previous observer is not usable, as the observability indices are now *at least* equal to 3, and that, the previous observer strategy, the observability indices must be lower or equal to 2. In this section, the observer is based on triangular form one.[25] Consider system (12) with the outputs $[y_1\ y_2]^T = [\delta_1\ \delta_2]^T$: an observability indices pair is $[k_1\ k_2]^T = [3\ 3]^T$, *i.e.* there exists $\mathcal{T}_{33} \subset \mathcal{X}$ such that, $\forall x \in \mathcal{T}_{33}$, $z = \Phi_{33}(x) = [z_1\ z_2\ z_3\ z_4\ z_5\ z_6]^T := [y_1\ \dot{y}_1\ \ddot{y}_1\ y_2\ \dot{y}_2\ \ddot{y}_2]^T$ is a state coordinates transformation. Under this latter transformation, system (12) can be rewritten as

$$\begin{aligned} \dot{z}_1 &= z_2 \\ \dot{z}_2 &= z_3 \\ \dot{z}_3 &= f_3(z) \\ \dot{z}_4 &= z_5 \\ \dot{z}_5 &= z_6 \\ \dot{z}_6 &= f_6(z) \\ y_1 &= z_1 \\ y_2 &= z_4 \end{aligned} \tag{31}$$

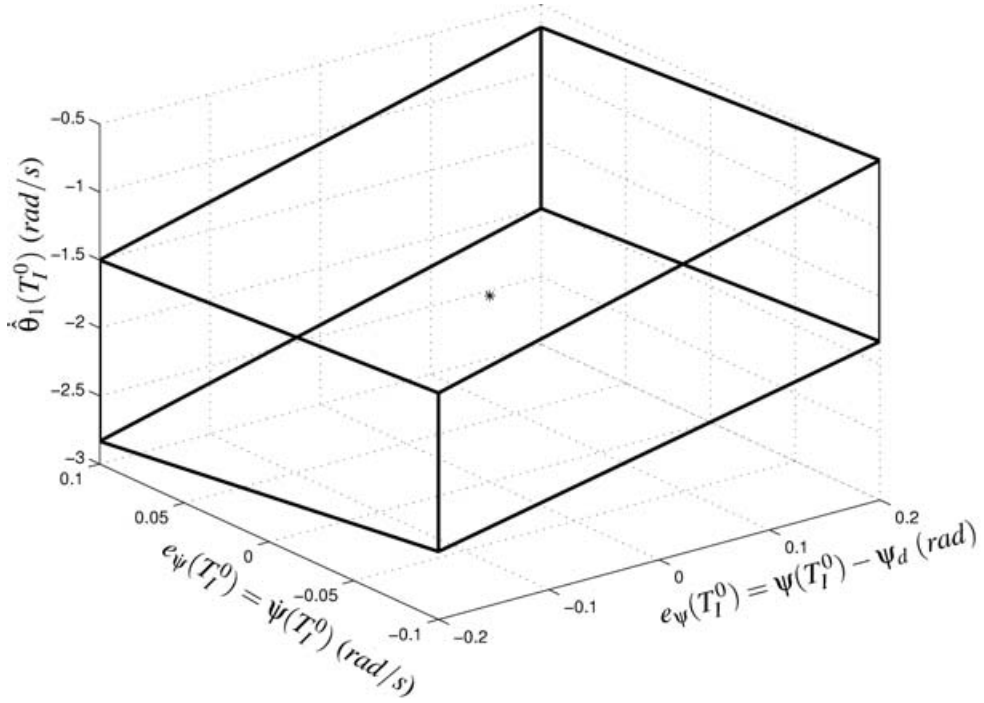

Fig. 8. $\dot{\hat{\theta}}_1^-(T_I^1)$ in terms of $e_\psi(T_I^0)$ and $e_{\dot{\psi}}(T_I^0)$. Each point of this 3D-area allows a convergence to the stable limit walking cycle. The star-point corresponds to the conditions for which the biped evolves on the stable limit cycle.

https://doi.org/10.1017/S0263574705002390 Published online by Cambridge University Press

IV.3.1. Observer design. An observer[25] for (31) reads as

$$\begin{array}{l}\dot{\hat{z}}_1 = \hat{z}_2 + E_1(t)\chi_1\\ \dot{\hat{z}}_2 = \hat{z}_3 + E_2(t)\chi_2\\ \dot{\hat{z}}_3 = f_3(\hat{z}) + E_3(t)\chi_3\\ \dot{\hat{z}}_4 = \hat{z}_5 + E_4(t)\chi_4\\ \dot{\hat{z}}_5 = \hat{z}_6 + E_5(t)\chi_5\\ \dot{\hat{z}}_6 = f_6(\hat{z}) + E_6(t)\chi_6\end{array} \tag{32}$$

with $\hat{z} := [\hat{z}_1\ \hat{z}_2\ \hat{z}_3\ \hat{z}_4\ \hat{z}_5\ \hat{z}_6]^T$ the estimated vector of z. Suppose that the initial error between the estimated and real vector is bounded. The principle of this class of observers consists in forcing, each in turn, estimated state variables to corresponding real ones, in finite time. The finite time convergence property is based on an adequate choice of $E_j(t)$ and χ_j ($j = \{1, \ldots, 6\}$), *i.e.* $E_j(t)$ and χ_j are defined such that each estimation error $e_j = \hat{z}_j - z_j$ converges to zero in finite time. One gets

- Function χ_i ($i = \{1, 4\}$) is based on the *twisting algorithm*[23] and reads as

$$\dot{\chi}_i = -\Lambda_i\ \text{sign}(\hat{z}_i - z_i) \tag{33}$$

with

$$\begin{array}{l}\Lambda_i = \begin{cases}\lambda_m^i & \text{if } e_i\dot{e}_i \le 0\\ \lambda_M^i & \text{if } e_i\dot{e}_i > 0\end{cases}\\ \lambda_m^i > \text{Max}(|e_{i+1}|)\\ \lambda_M^i > 3\lambda_m^i\end{array} \tag{34}$$

- Function χ_j ($j = \{2, 3, 5, 6\}$) uses the standard sliding mode approach and reads as

$$\chi_j = -\lambda_j\ \text{sign}(\hat{z}_j - \tilde{z}_j) \tag{35}$$

with $\lambda_j > 0$, and

$$\tilde{z}_j = \hat{z}_j + E_{j-1}(t)\chi_{j-1} \tag{36}$$

The estimation error dynamics is

$$\begin{array}{l}\dot{e}_1 = e_2 + E_1(t)\chi_1\\ \dot{e}_2 = e_3 + E_2(t)\chi_2\\ \dot{e}_3 = f_3(\hat{z}) - f_3(z) + E_3(t)\chi_3\\ \dot{e}_4 = e_4 + E_4(t)\chi_4\\ \dot{e}_5 = e_5 + E_5(t)\chi_5\\ \dot{e}_6 = f_6(\hat{z}) - f_6(z) + E_6(t)\chi_6\end{array} \tag{37}$$

with $e_j = \hat{z}_j - z_j$, $j = \{1, \ldots, 6\}$. The following steps display the determination of E_j and the proof of finite time convergence.

- **Step 1.** Suppose that $e_1^i(0) \neq 0$ ($i = \{1, 4\}$). Observer (32) is initialized such that $E_1 = E_4 = 1$ and $E_2 = E_3 = E_5 = E_6 = 0$. The error dynamics reads as

$$\begin{array}{l}\dot{e}_1 = e_2 + \chi_1\\ \dot{e}_2 = e_3\\ \dot{e}_3 = f_3(\hat{z}) - f_3(z)\\ \dot{e}_4 = e_5 + \chi_4\\ \dot{e}_5 = e_6\\ \dot{e}_6 = f_6(\hat{z}) - f_6(z)\end{array} \tag{38}$$

As χ_j is based on the twisting algorithm with appropriate tuning of Λ_j, e_j ($j = \{1, 4\}$) reaches zero in finite time at $t = t_j$. Then, $\forall\ t \ge t_j$, $e_j(t) = \dot{e}_j(t) = 0$, *i.e.*

$$e_j = 0 \quad \dot{e}_j = e_{j+1} + \chi_j = \hat{z}_{j+1} - z_{j+1} + \chi_j = 0 \tag{39}$$

From (39), one gets $\hat{z}_{j+1} + \chi_j = z_{j+1}$ and from (36), $z_{j+1} = \tilde{z}_{j+1}$.

- **Step 2.** For $t \ge t_j$, one states $E_j = E_{j+1} = 1$ and $E_3 = E_6 = 0$. From (35)–(39), dynamics of e_2, e_3, e_5 and e_6 read as

$$\begin{array}{l}\dot{e}_2 = e_3 - \lambda_2\ \text{sign}(e_2)\\ \dot{e}_3 = f_3(\hat{z}) - f_3(z)\\ \dot{e}_5 = e_6 - \lambda_5\ \text{sign}(e_5)\\ \dot{e}_6 = f_6(\hat{z}) - f_6(z)\end{array} \tag{40}$$

By tuning $\lambda_i > \text{Max}(|e_{i+1}|)$ ($i = \{2, 5\}$), a finite time convergence to $e_i = 0$ is ensured at $t = t_i$. Then, $\forall\ t \ge t_i$, $e_i(t) = \dot{e}_i(t) = 0$, *i.e.*

$$\begin{array}{ll}e_1 = 0 & \dot{e}_1 = 0\\ e_2 = 0 & \dot{e}_2 = e_3 + \chi_2 = 0\\ e_4 = 0 & \dot{e}_4 = 0\\ e_5 = 0 & \dot{e}_5 = e_6 + \chi_5 = 0\end{array} \tag{41}$$

From the second line of (41), one gets $\hat{z}_{i+1} + \chi_i = z_{i+1}$ and from (36), $z_{i+1} = \tilde{z}_{i+1}$.

- **Step 3.** For $t \ge t_i$, one states $E_j = 1$ ($j = \{1, \ldots, 6\}$). From (35)–(41), dynamics of e_3 and e_6 reads as

$$\begin{array}{l}\dot{e}_3 = f_3(\hat{z}) - f_3(z) - \lambda_3\ \text{sign}(\hat{z}_3 - z_3)\\ \dot{e}_6 = f_6(\hat{z}) - f_6(z) - \lambda_6\ \text{sign}(\hat{z}_6 - z_6)\end{array} \tag{42}$$

By tuning $\lambda_i > \text{Max}(|f_i(\hat{z}) - f_i(z)|)$ ($i = \{3, 6\}$), a finite time convergence to $e_i = 0$ is ensured, which implies a finite time convergence of the observer.

Then, a finite time convergence observer for (32) reads as

$$\dot{\hat{z}} = A_{33}\hat{z} + F_{33}(\hat{z}) + \chi_{33}(\cdot) \tag{43}$$

with

$$A_{33} := \left[\begin{array}{ccc|ccc}0 & 1 & 0 & 0 & 0 & 0\\ 0 & 0 & 1 & 0 & 0 & 0\\ 0 & 0 & 0 & 0 & 0 & 0\\ \hline 0 & 0 & 0 & 0 & 1 & 0\\ 0 & 0 & 0 & 0 & 0 & 1\\ 0 & 0 & 0 & 0 & 0 & 0\end{array}\right] \quad F_{33}(\hat{z}) := \left[\begin{array}{c}0\\ 0\\ f_3(\hat{z})\\ \hline 0\\ 0\\ f_6(\hat{z})\end{array}\right]$$

https://doi.org/10.1017/S0263574705002390 Published online by Cambridge University Press

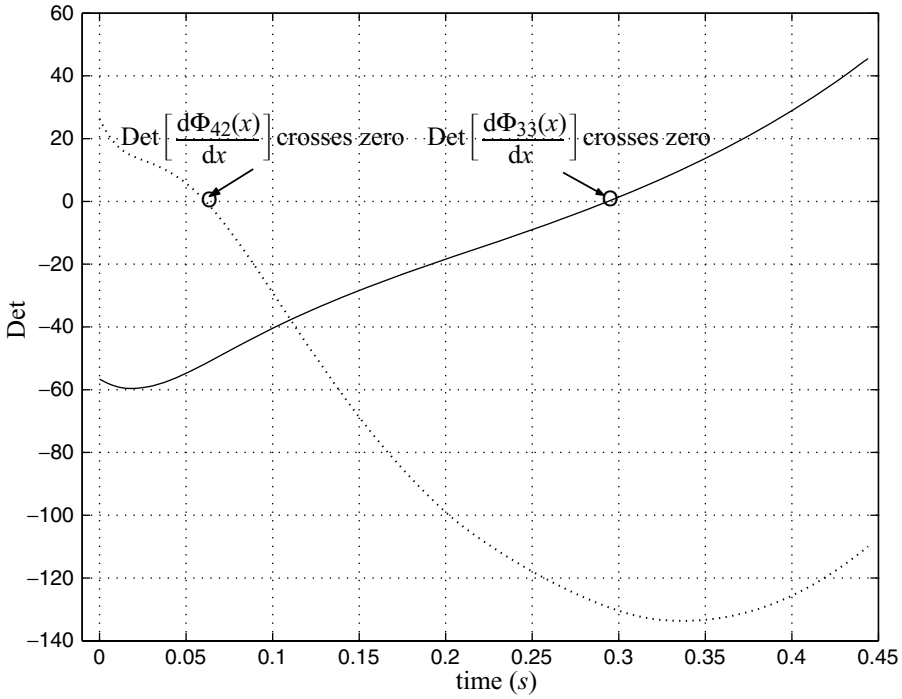

Fig. 9. Det$[\frac{d\Phi_{33}(x)}{dx}]$ (Bold line) and Det$[\frac{d\Phi_{42}(x)}{dx}]$ (Dotted line) versus time (s.) over one step.

$$\chi_{33}(\cdot) := \begin{bmatrix} E_1\chi_1 \\ E_2\chi_2 \\ E_3\chi_3 \\ \hline E_4\chi_4 \\ E_5\chi_5 \\ E_6\chi_6 \end{bmatrix} = \begin{bmatrix} -E_1\Lambda_1\ \mathrm{sign}(\hat{z}_1 - y_1) \\ -E_2\lambda_2\ \mathrm{sign}(\hat{z}_2 - \tilde{z}_2) \\ -E_3\lambda_3\ \mathrm{sign}(\hat{z}_3 - \tilde{z}_3) \\ \hline -E_4\Lambda_4\ \mathrm{sign}(\hat{z}_4 - y_2) \\ -E_5\lambda_5\ \mathrm{sign}(\hat{z}_5 - \tilde{z}_5) \\ -E_6\lambda_6\ \mathrm{sign}(\hat{z}_6 - \tilde{z}_6) \end{bmatrix}$$

Loss of observability

During the swing phase, along the *nominal* trajectories, Det$[\frac{d\Phi_{33}(x)}{dx}]$ crosses zero (see Figure 9). Of course, as in the previous case, it induces a problem for the observer design. A solution, *which could not be used in the previous case*, is to design the observer with an other pair of observability indices. As a matter of fact, $\{k_1, k_2\} = \{4, 2\}$ is also eligible: there exists $\mathcal{T}_{42} \subset \mathcal{X}$ such that, $\forall x \in \mathcal{T}_{42}$, the function $z = \Phi_{42}(x) = [z_1\ z_2\ z_3\ z_4\ z_5\ z_6]^T := [y_1\ \dot{y}_1\ \ddot{y}_1\ y_1^{(3)}\ y_2\ \dot{y}_2]^T$ is a state transformation. The same observer design approach then previously is used for the design of a finite time convergence observer with $\{k_1, k_2\} = \{4, 2\}$; then, one gets

$$\dot{\hat{z}} = A_{42}\hat{z} + F_{42}(\hat{z}) + \chi_{42}(\cdot) \tag{44}$$

with

$$A_{42} := \left[\begin{array}{cccc|cc} 0 & 1 & 0 & 0 & 0 & 0 \\ 0 & 0 & 1 & 0 & 0 & 0 \\ 0 & 0 & 0 & 1 & 0 & 0 \\ 0 & 0 & 0 & 0 & 0 & 0 \\ \hline 0 & 0 & 0 & 0 & 0 & 1 \\ 0 & 0 & 0 & 0 & 0 & 0 \end{array}\right] \quad F_{42}(\hat{z}) := \begin{bmatrix} 0 \\ 0 \\ 0 \\ f_4(\hat{z}) \\ \hline 0 \\ f_6(\hat{z}) \end{bmatrix}$$

$$\chi_{42}(\cdot) := \begin{bmatrix} E_1\chi_1 \\ E_2\chi_2 \\ E_3\chi_3 \\ E_4\chi_4 \\ \hline E_5\chi_5 \\ E_6\chi_6 \end{bmatrix} = \begin{bmatrix} -E_1\Lambda_1\ \mathrm{sign}(\hat{z}_1 - y_1) \\ -E_2\lambda_2\ \mathrm{sign}(\hat{z}_2 - \tilde{z}_2) \\ -E_3\lambda_3\ \mathrm{sign}(\hat{z}_3 - \tilde{z}_3) \\ -E_4\lambda_4\ \mathrm{sign}(\hat{z}_4 - \tilde{z}_4) \\ \hline -E_5\Lambda_5\ \mathrm{sign}(\hat{z}_5 - y_2) \\ -E_6\lambda_6\ \mathrm{sign}(\hat{z}_6 - \tilde{z}_6) \end{bmatrix}$$

For this latter choice of observability indices, there is also loss of observability but not in the same conditions than previously (see Figure 9). Then, the observation strategy can be described as follows:

Observation algorithm

Let $T_{SW} := \mathrm{Min}(t)$ such that $t \in [T_I^i, T_I^{i+1}]$ and Det$[\frac{d\Phi_{33}(x)}{dx}](t) = 0$. Then, one has

- For $t \in [T_I^i, T_{SW}]$, the observer is designed with $\{k_1, k_2\} = \{3, 3\}$,
- From $t \in [T_{SW}, T_I^{i+1}]$, the observer is designed with $\{k_1, k_2\} = \{4, 2\}$. ■

The following proposition displays the design of a finite time convergence observer for (11).

Proposition 5. *A finite time convergence observer for the nonlinear system* (11) *reads as*

$$\dot{\hat{x}} = f(\hat{x}) + g(y)\Gamma + M\chi(\cdot) \tag{45}$$

with

$$M\chi(\cdot) = \begin{cases} \left[\frac{d\Phi_{33}(\hat{x})}{d\hat{x}}\right]^{-1} \chi_{33} & \text{for } t \in [T_I^i, T_{SW}] \quad \text{then } \hat{x} \in \mathcal{T}_{33} \\ \left[\frac{d\Phi_{42}(\hat{x})}{d\hat{x}}\right]^{-1} \chi_{42} & \text{for } t \in [T_{SW}, T_I^{i+1}] \quad \text{then } \hat{x} \in \mathcal{T}_{42} \end{cases} \tag{46}$$

https://doi.org/10.1017/S0263574705002390 Published online by Cambridge University Press

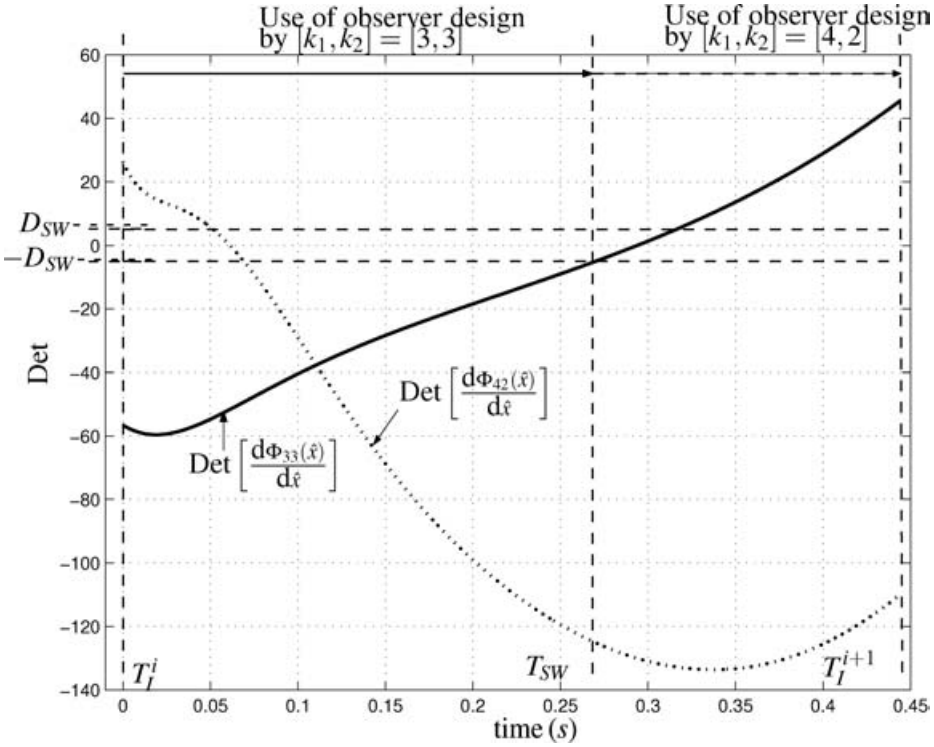

Fig. 10. Det$[\frac{d\Phi_{33}(\hat{x})}{d\hat{x}}]$ (Bold line) and Det$[\frac{d\Phi_{42}(\hat{x})}{d\hat{x}}]$ (Dotted line) versus time (s.) over one step.

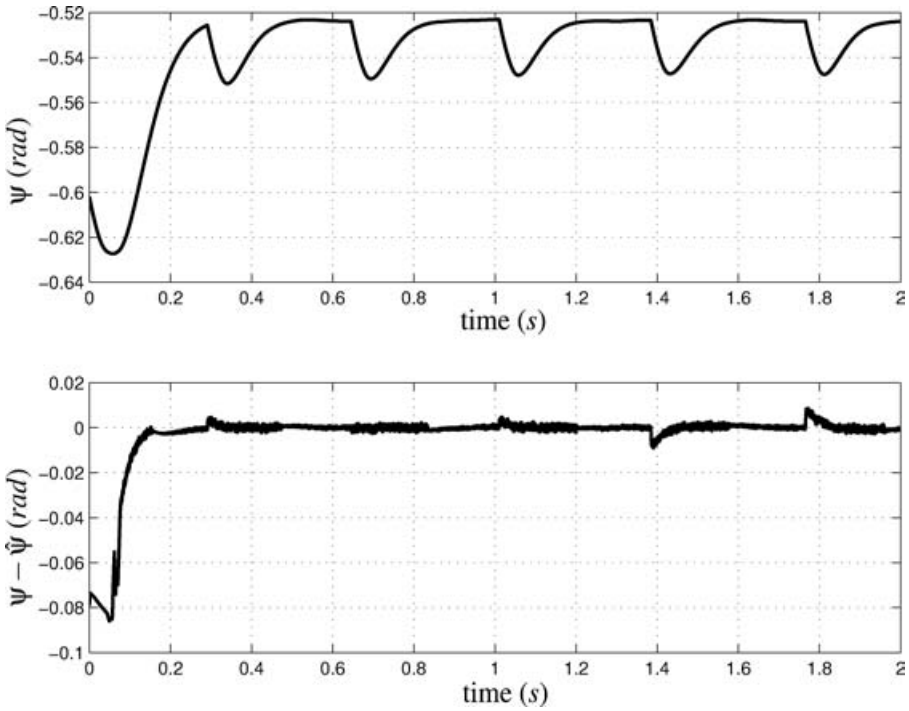

Fig. 11. Absolute orientation ψ (rad) (top), estimation error $\psi - \hat{\psi}$ (rad) (bottom) versus time (sec.).

with T_I^i the initial impact time of the step, T_I^{i+1} the impact time at the end of the step, and $T_{SW} := \text{Min}(t)$ such that $t \in [T_I^i, T_I^{i+1}]$ and Det$[\frac{d\Phi_{33}(\hat{x})}{d\hat{x}}](t) = 0$.

Practical point-of-view

- *The commutation from the first observer structure to the second one is made through the condition that $T_{SW} :=$ Min(t) such that $t \in [T_I^i, T_I^{i+1}]$ and $|\text{Det}[\frac{d\Phi_{33}(\hat{x})}{d\hat{x}}]|(t) = D_{SW}$, where $D_{SW} > 0$ a real fixed by the user (see Figure 10). The choice of D_{SW} is made in order that the condition number with respect to inversion of $[\frac{d\Phi_{33}(\hat{x})}{d\hat{x}}]$ is not "too much large".*
- *The finite-time convergence observer previously exposed ensures that the estimation errors exactly converge to zero. In practice, this property is ensured for a neighborhood*

https://doi.org/10.1017/S0263574705002390 Published online by Cambridge University Press

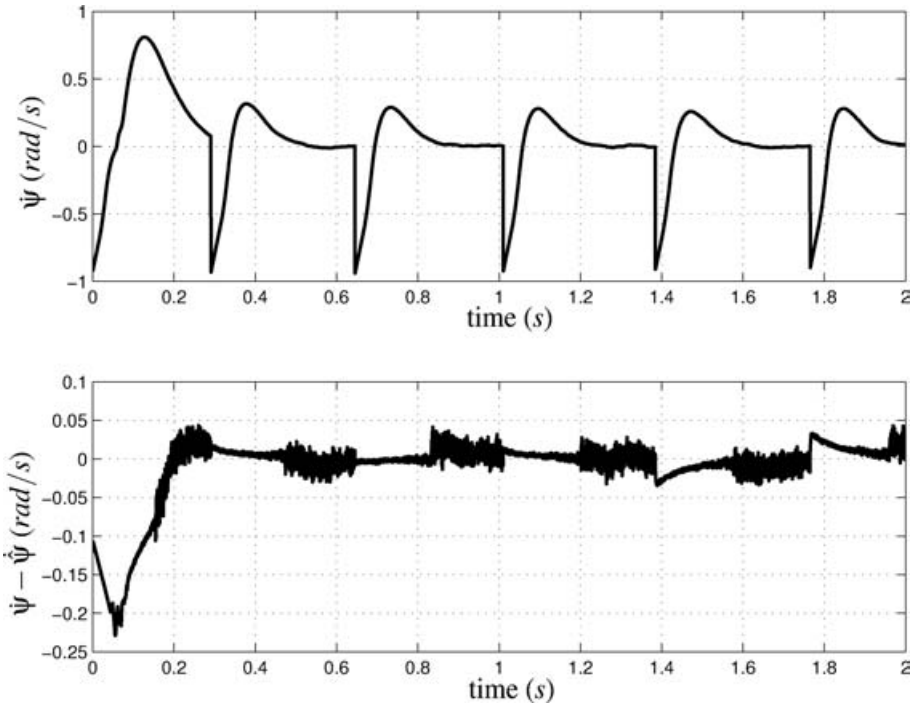

Fig. 12. Absolute velocity $\dot{\psi}$ (rad/s) (top), estimation error $\dot{\psi} - \hat{\dot{\psi}}$ (rad/s) (bottom) versus time (sec.).

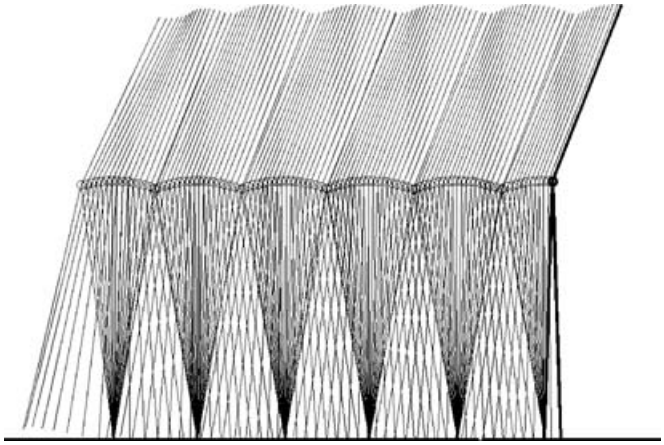

Fig. 13. Plot of walking as a sequence of stick figure.

of zero[25] *which the estimation errors are forced to reach and to stay in*.

IV.3.2. Simulations. The control law described in Section III is tuned with $\alpha = 0.9$ and $\epsilon = 20$. The desired value for ψ is stated as $\psi_d = -0.5236$ rad. The value δ_{2f}, which defines the length of the step and also the impact event, is stated as $\delta_{2f} = -2.3562$ rad. The parameter D_{SW} has been tuned to 5. For $\{k_1, k_2\} = \{3, 3\}$ and $\{k_1, k_2\} = \{4, 2\}$ the observer parameters are respectively

- $\lambda_m^1 = 2,\ \lambda_M^1 = 10,\ \lambda_2 = 2,\ \lambda_3 = 60,\ \lambda_m^4 = 2,\ \lambda_M^4 = 10,\ \lambda_5 = 2, \lambda_6 = 10$
- $\lambda_m^1 = 2,\ \lambda_M^1 = 10,\ \lambda_2 = 2,\ \lambda_3 = 60,\ \lambda_4 = 600,\ \lambda_m^5 = 2,\ \lambda_M^5 = 10, \lambda_6 = 2$

The observer and the control law parameters have been tuned such that the observer convergence time is smaller than the control law convergence time, which is smaller than the impact event. The initial real and estimated values have been, respectively, stated as

$$\begin{aligned}&\left[\dot{\delta}_1(0), \dot{\delta}_2(0), \dot{\psi}(0), \delta_1(0),\ \delta_2(0), \psi(0)\right]\\ &\quad = [-1.725, 1.725, 0.0, -2.8798, -2.3562, -0.6021]\\ &\left[\hat{\dot{\delta}}_1(0), \hat{\dot{\delta}}_2(0), \hat{\dot{\psi}}(0), \hat{\delta}_1(0), \hat{\delta}_2(0), \hat{\psi}(0)\right]\\ &\quad = [-1.500, 1.500, 0.0, -2.8798, -2.3562, -0.5236]\end{aligned}$$

One supposes that there are initial estimation errors on absolute variable and also on the relative velocities, which are not measured, and that these initial (estimated and real) state variables have been stated such that the biped robot reachs a stable walking cycle.[33] Figure 11 displays absolute position and the corresponding estimation error which converges to zero before each impact. This is also the case for $\dot{\psi}$ and its estimation error $\dot{\psi} - \hat{\dot{\psi}}$ (Figure 12). The control law has been tuned such that the control output vector y equals zero before the impact (ψ reachs desired value ψ_d, see Figure 11-top), and the biped reaches a stable periodic cycle after several steps (see Figures 13 and 14). As shown by Figure 14, during the first step, two phenomena are acting. First, the estimated state variables are converging to real values which induces a large transient over the first step only (as the observer is tuned such that the estimation error equals zero before the end of the first step). Once the observer has converged, the control law ensures that the biped robot reachs a stable walking cycle, as the initial conditions have been adequately chosen.

https://doi.org/10.1017/S0263574705002390 Published online by Cambridge University Press

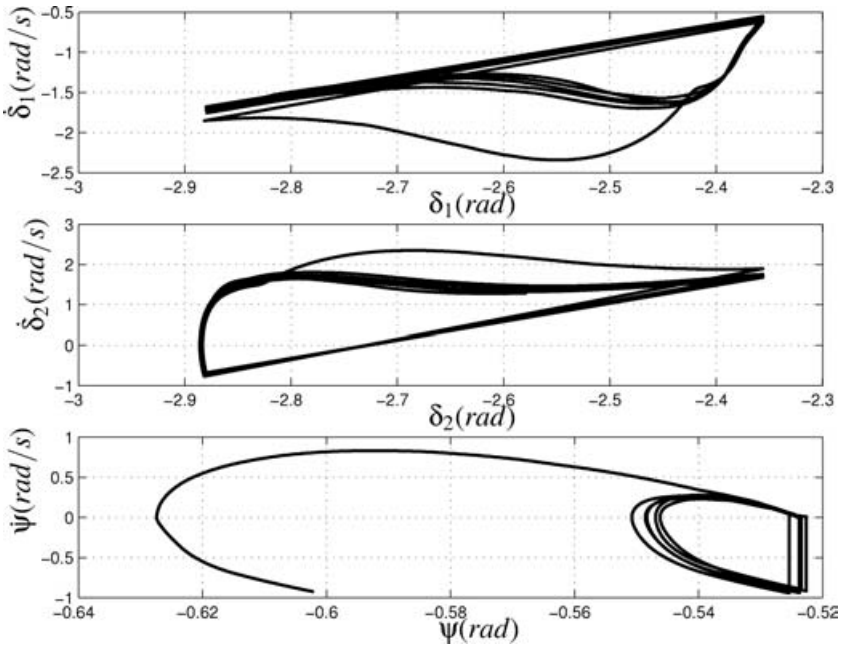

Fig. 14. Phase plan $(\dot{\delta}_1, \delta_1)$, $(\dot{\delta}_2, \delta_2)$ and $(\dot{\psi}, \psi)$.

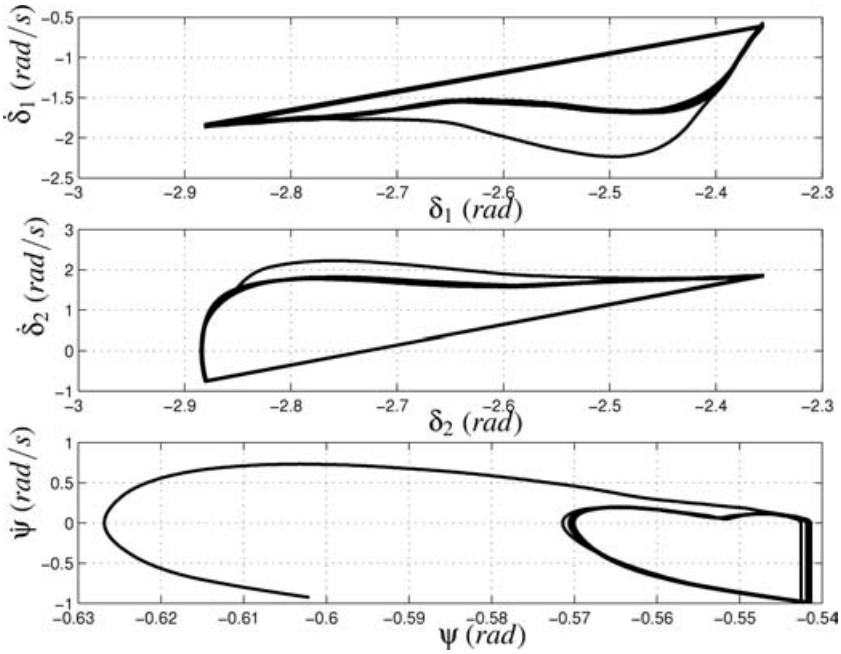

Fig. 15. Phase plan $(\dot{\delta}_1, \delta_1)$, $(\dot{\delta}_2, \delta_2)$ and $(\dot{\psi}, \psi)$, effect of a Coulomb friction.

In order to evaluate the robustness properties of the observer, a numerical test has been realized with an additive Coulomb friction in the biped model. These frictions are essentially located in the gearbox reducers. Then, model (2) is modified such as

$$D\ddot{q} + C\dot{q} + G = B\Gamma - \Gamma_{rot}\text{sign}(\dot{q}_{rel}) \qquad (47)$$

The design of observers and control law does not take into account the Coulomb friction. Therefore, this friction is acting as a perturbation for robustness tests. The nominal value of the Coulomb friction is $\Gamma_{rot} = 2$ N · m. The initial real and estimated values are defined by (47). Figure 15 displays walking cycles over several steps. The walking gait converges to a stable cycle, which characterizes the robustness of the observer-based control.

V. CONCLUSION

The measure of the absolute orientation of mobile robots such as dynamically stable biped is difficult to obtain. However its knowledge is useful for the control during the locomotion. Then we proposed in this paper, a solution, based on the observation of the state vector. Two observers are designed

https://doi.org/10.1017/S0263574705002390 Published online by Cambridge University Press

to estimate the absolute orientation of a biped, one from the knowledge of actuated positions and velocity and one from the knowledge of actuated joint variables only, for a walking gait composed of single-supports and impacts. The main property of the observers and the control law is the finite-time convergence, which allows to ensure its convergence before each impact and provide the existence of a cyclic gait. Then, these observers are well adapted to the problem of the cyclic gait. The observers coupled with a finite time convergence controller induce an attraction basin, from which stable walking gait establishment is possible and proved. The fact leads to think that experiments with a prototype are realistic. The future objectives consist to extend these results to a five link biped prototype.

References

1. M. Vukobratovic and D. Juricic, "Contribution to the synthesis of biped gait," *Proc. of the IFAC Symp. Technical and Biological on Control*, Erevan, USSR (1968). pp. 1–6.
2. M. Vukobratovic, D. Surla and D. Stokic, *Biped Locomotion* (Springer-Verlag, 1990).
3. M. Vukobratovic and B. Borovac, "Zero-moment pont-thirty five years of its life," *International Journal of Humanoid Robotics* **1**(1), 157–173 (2004).
4. V. V. Beletskii and P. S. Chudinov, "Parametric optimization in the problem locomotion," *Izv. An SSSR Mekhanika Tverdovo Tela* [Mechanics of Solids] **1**, 25–35 (2001).
5. A. M. Formal'sky, *Locomotion of Anthropomorphic Mechanisms* (Nauka, Moscow [In Russian], 1982).
6. I. E. Sutherland and M. H. Raibert, "Machines that walk," *Scientific American* **248**, 44–53 (1983).
7. K. Hirai, M. Hirose and T. Haikawa, "The development of honda humanoid robot," *Proc. of the IEEE Conf. on Robotics and Automation* (1998) pp. 1321–1326.
8. K. Kaneko, F. Kanehiro, S. Kajita, H. Hirukawa, T. Kawasaki, M. Hirata, K. Akachi and T. Isozumi, "Humanoid robot hrp-2," *Proc. of the IEEE Conf. on Robotics and Automation* (2004) pp. 1083–1090.
9. C. Chevallereau and Y. Aoustin, "Optimal reference trajectories for walking and running of a biped," *Robotica* **19**, (5), 557–569 (2001).
10. A. Muraro, C. Chevallereau and Y. Aoustin, "Optimal trajectories for a quadruped robot with trot, amble and curvet gaits for two energetic criteria," *Multibody System Dynamics* (Kluwer Academic Publishers) **9**(3), 39–62 (2003).
11. Y. Hurmuzlu, F. Génot and B. Brogliato, "Modeling, stability and control of biped robots-a general framework," *Automatica* **10**, 1647–1664 (2004).
12. P. H. Channon, S. H. Hopkins and D. T. Pham, "Derivation of optimal walking motions for a bipedal walking robot," *Robotica* **2**, 165–172 (1992).
13. C. Sabourin, O. Bruneau and J. G. Fontaine, "Pragmatic rules for real-time control of the dynamic walking of an under-actuated biped robot," *Proc. of the IEEE Conf. on Robotics and Automation* (2004) pp. 4216–4222.
14. F. Zonfrilli, M. Oriolo and T. Nardi, "A biped locomotion strategy for the quadruped robot sony ers-210," *Proc. of the IEEE Conf. on Robotics and Automation* (2002) pp. 2768–2774.
15. C. Chevallereau, G. Abba, Y. Aoustin, F. Plestan, E. R. Westervelt, C. Canudas de Wit and J.W. Grizzle, "Rabbit: a testbed for advanced control theory," *IEEE Control Systems Magazine* **23**(5), 57–79 (2003).
16. P. Micheau, M. A. Roux and P. Bourassa, "Self-tuned trajectory control of a biped walking robot," *Proc. International Conference on Climbing and Walking Robot*, Catania, Italy (2003) pp. 527–534.
17. V. Lebastard, Y. Aoustin and F. Plestan, "Observer-based control of a biped robot," *Proc. Fourth International Workshop on Robot Motion and Control*, Puszczykowo, Poland (2004) pp. 67–72.
18. G. Bornard and H. Hammouri, "A high gain observer for a class of uniformly observable systems," *Proceedings of 30th Conference on Decision and Control* (1991) pp. 1494–1496.
19. J. P. Gauthier and G. Bornard, "Observablity for any $u(t)$ of a class of nonlinear systems," *IEEE Transactions on Automatic Control* **26**(4), 922–926 (1981).
20. Y. Aoustin, G. Garcia and A. Janot, "Estimation of the absolute orientation of a two-link biped using discrete observers," *Proc. of the conference Mechatronics and Robotics, Leuven, Belgium* (2004) pp. 1315–1320.
21. R. E. Kalman, P. L. Falb and M. A. Arbib, *Topics in Mathematical System Theory* (Mc Graw-Hill Book Company, 1969).
22. J. J. E. Slotine and W. Li, *Applied Nonlinear Control* (Prentice Hall International, 1991).
23. A. Levant, "Sliding order and sliding accuracy in sliding mode control," *International Journal of Control* **58**(6), 1247–1263 (1993).
24. T. Floquet, J. P. Barbot and W. Perruquetti, "A finite time observer for flux estimation in the induction machine," *Proc. IEEE Conference on Control Applications*, Glasgow, Scotland (2002) pp. 335–339.
25. T. Boukhobza and J. P. Barbot, "High order sliding modes observer," *Proc. IEEE Conference on Decision and Control*, Tampa, Florida USA (1998) pp. 1912–1917.
26. J. W. Grizzle, G. Abba and F. Plestan, "Asymptotically stable walking for biped robots: analysis via systems with impulse effects," *IEEE Transactions on Automatic Control* **46**(1), 51–64 (2001).
27. Y. Hurmuzlu and D. B. Marghitu, "Rigid body collisions of planar kinematic chains with multiple contact points," *The International Journal of Robotics Research* **13**(1), 82–92 (1994).
28. M. W. Spong and M. Vidyasagar, *Robots Dynamics and Control* (John Wiley, 1989).
29. A. Isidori, *Nonlinear Control Systems* (Springer, 1995).
30. S. P. Bhat and D. S. Bernstein, "Continuous finite-time stabilization of the translational and rotationnal double integrator," *IEEE Transaction on Automatic Control* **43**(5), 678–682 (1998).
31. Menini L. and A. Tornambè, "Velocity observers for linear mechanical systems subject to single non-smooth impacts," *Systems and Control Letters* **43**, 193–202 (2001).
32. F. Plestan, J. W. Grizzle, E. R. Westervelt and G. Abba, "Stable walking of a 7-dof biped robot," *IEEE Transactions on Robotics and Automation* **19**(4), 653–668 (2003).
33. V. Lebastard, Y. Aoustin and F. Plestan, "Second order sliding mode observer for stable control of a walking biped robot," *IFAC World Congress* (2005) CD–Rom.

APPENDIX

A. DYNAMIC MODEL IN SINGLE SUPPORT PHASE

$$
\begin{aligned}
D_{11} &= N^2 I - 2m_1 L_1 s_1 + I_1 + m_1 L_1^2 + m_1 s_1^2 \\
&\quad + m_2 L_1^2 + m_3 L_1^2 \\
D_{12} &= D_{21} = -m_2 s_2 L_1 \cos(\delta_1 - \delta_2) \\
D_{13} &= D_{31} = m_1 L_1^2 - m_3 L_1 s_3 \cos(\delta_1) + m_3 L_1^2 + m_2 L_1^2 \\
&\quad - 2m_1 L_1 s_1 + I_1 - m_2 s_2 L_1 \cos(\delta_1 - \delta_2) + m_1 s_1^2 \\
D_{22} &= m_2 s_2^2 + I_2 + N^2 I \\
D_{23} &= D_{32} = -m_2 s_2 L_1 \cos(\delta_1 - \delta_2) + m_2 s_2^2 + I_2 \\
D_{33} &= m_1 L_1^2 - 2m_3 L_1 s_3 \cos(\delta_1) + m_3 L_1^2 + m_2 L_1^2 \\
&\quad - 2m_1 L_1 s_1 + I_1 + I_2 + I_3 + m_2 s_2^2 \\
&\quad - 2m_2 s_2 L_1 \cos(\delta_1 - \delta_2) + m_1 s_1^2 + m_3 s_3^2
\end{aligned}
$$

https://doi.org/10.1017/S0263574705002390 Published online by Cambridge University Press

$$
\begin{aligned}
H_{12} &= -m_2 s_2 L_1 \sin(\delta_1 - \delta_2)(\dot{\psi} + \dot{\delta}_2) \\
H_{13} &= -L_1(m_2 s_2 \sin(\delta_1 - \delta_2)\dot{\delta}_2 + \dot{\psi} m_3 s_3 \sin(\delta_1) \\
&\quad + m_2 s_2 \sin(\delta_1 - \delta_2)\dot{\psi}) \\
H_{21} &= m_2 s_2 L_1 \sin(\delta_1 - \delta_2)(\dot{\psi} + \dot{\delta}_1) \\
H_{23} &= m_2 s_2 L_1 \sin(\delta_1 - \delta_2)(\dot{\psi} + \dot{\delta}_1) \\
H_{31} &= L_1(m_3 s_3 \sin(\delta_1) + m_2 s_2 \sin(\delta_1 - \delta_2))(\dot{\psi} + \dot{\delta}_1) \\
H_{32} &= -m_2 s_2 L_1 \sin(\delta_1 - \delta_2)(\dot{\psi} + \dot{\delta}_2) \\
H_{33} &= L_1(\dot{\delta}_1 m_3 s_3 \sin(\delta_1) + m_2 s_2 \sin(\delta_1 - \delta_2)\dot{\delta}_1 \\
&\quad - m_2 s_2 \sin(\delta_1 - \delta_2)\dot{\delta}_2)
\end{aligned}
$$

$$
\begin{aligned}
G_1 &= g\sin(\psi + \delta_1)(m_1 L_1 - m_1 s_1 + m_2 L_1 + L_1 m_3) \\
G_2 &= -g m_2 s_2 \sin(\psi + \delta_2) \\
G_3 &= g(m_1 \sin(\psi + \delta_1) L_1 - m_1 \sin(\psi + \delta_1) s_1 \\
&\quad + m_2 L_1 \sin(\psi + \delta_1) - m_2 s_2 \sin(\psi + \delta_2) \\
&\quad + m_3 L_1 \sin(\psi + \delta_1) - m_3 s_3 \sin(\psi))
\end{aligned}
$$

$$
B = \begin{bmatrix} 1 & 0 \\ 0 & 1 \\ 0 & 0 \end{bmatrix} \tag{48}
$$

Remark 3. *The symmetric positive inertia matrix D is independent of the absolute orientation of the biped (ψ).*

B. IMPACT MODEL

The impact equations 4 and an additional set of two equations is obtained from the condition that the swing leg does not rebound or not slip at impact, $D_R \dot{q}_e^+ = 0$ become

$$
\begin{bmatrix} D_e & -D_R^T \\ D_R & 0_{2\times 2} \end{bmatrix} \begin{bmatrix} \dot{q}_e^+ \\ R \end{bmatrix} = \begin{bmatrix} D_e \dot{q}_e^- \\ 0 \end{bmatrix} \tag{49}
$$

where $R = [R_{N_1}\ R_{T_1}\ R_{N_2}\ R_{T_2}]^T$,

$$
\begin{aligned}
D_{e11} &= m_1 s_1^2 + I_1 + N^2 I \\
D_{e13} &= D_{e31} = -m_1 s_1 s_3 \cos(\delta_1) + m_1 s_1^2 + I_1 \\
D_{e14} &= D_{e41} = -m_1 s_1 \cos(\psi + \delta_1) \\
D_{e15} &= D_{e51} = -m_1 s_1 \sin(\psi + \delta_1) \\
D_{e22} &= m_2 s_2^2 + I_2 + N^2 I \\
D_{e23} &= D_{e32} = -m_2 s_2 s_3 \cos(\delta_2) + m_2 s_2^2 + I_2 \\
D_{e24} &= D_{e42} = -m_2 s_2 \cos(\psi + \delta_2) \\
D_{e25} &= D_{e52} = -m_2 s_2 \sin(\psi + \delta_2) \\
D_{e33} &= I_1 + m_1 s_1^2 + m_1 s_3^2 + m_2 s_3^2 \\
&\quad - 2m_1 s_1 s_3 \cos(\delta_1) - 2m_2 s_2 s_3 \cos(\delta_2) + m_2 s_2^2 + I_2 + I_3 \\
D_{e34} &= D_{e43} = m_1 s_3 \cos(\psi) - m_1 s_1 \cos(\psi + \delta_1) \\
&\quad + m_2 s_3 \cos(\psi) - m_2 s_2 \cos(\psi + \delta_2) \\
D_{e35} &= D_{e53} = m_1 s_3 \sin(\psi) - m_1 s_1 \sin(\psi + \delta_1) \\
&\quad + m_2 s_3 \sin(\psi) - m_2 s_2 \sin(\psi + \delta_2) \\
D_{e44} &= m_1 + m_2 + m_3 \\
D_{e55} &= m_1 + m_2 + m_3
\end{aligned}
$$

$$
\begin{aligned}
&D_R^T \\
&= \begin{bmatrix} 0 & -L_2\cos(\psi + \delta_2) & s_3\cos(\psi) - L_2\cos(\psi + \delta_2) & 1 & 0 \\ 0 & -L_2\sin(\psi + \delta_2) & s_3\sin(\psi) - L_2\sin(\psi + \delta_2) & 0 & 1 \end{bmatrix}
\end{aligned} \tag{50}
$$

$$
\Delta(x^-) = [q_2^-\ q_1^-\ q_3^-\ \dot{q}_2^+\ \dot{q}_1^+\ \dot{q}_3^+].
$$

Remark 4. *At an impulsive impact the configuration of the biped is invariant.*

https://doi.org/10.1017/S0263574705002390 Published online by Cambridge University Press